**This is a clear manuscript that cleanly demonstrates the utility of Brutsaert's equation for calculating DLR from two easily observable state variables (two meter air temperature and vapor pressure). I had never heard of Brutsaert's empirical equation before reading this paper, and the manuscript gave some nice physical insights on DLR variations across time and space.**

We thank the reviewer for his appreciation of our work and constructive comments. The reviewer suggested some important points that need more clarity. We have now accordingly revised the manuscript with the point-by-point response mentioned in this document. The reviewer comments are shown in bold blue and our responses are shown in black. And the italic text in Times New Roman style is what we revised in the text.

**One major question I have is, how does Brutsaert's equation compare to radiative kernels, which have been used by a few recent studies (e.g. Shakespeare & Roderick 2022 and Vargas Zeppetello et al. 2019) to attribute changes in DLR to changes in near-surface state variables? This might help give Brustaert's equation a more interpretable physical intuition, because the kernels are calculated via climate models and their radiative transfer schemes.**

[Reply] Thank the reviewer for the constructive comment. As suggested, we have now used radiative kernels as described in Vargas Zeppetello et al. (2019) and Shakespeare & Roderick (2022) to understand the sensitivity in the estimated downwelling longwave radiation for the seasonal change in the atmospheric property ($T_a$, $e_a$, and $f_c$), i.e., $\frac{\partial R_{ld}}{\partial T} = 4\sigma\bar{\varepsilon}\bar{T}_a^{\,3}$, $\frac{\partial R_{ld}}{\partial f_c} = \sigma\bar{T}_a^{\,4} \times \left(1 - \overline{1.24\left(\frac{\bar{e}_a}{\bar{T}_a}\right)^{\frac{1}{7}}}\right)$, and $\frac{\partial R_{ld}}{\partial e_a} = \sigma\bar{T}_a^{\,4} \times \frac{1.24}{7}\frac{(1-\bar{f}_c)}{(\bar{e}_a)^{\frac{6}{7}}(\bar{T}_a)^{\frac{1}{7}}}$. The results are shown in Figure R1, together with the seasonal cycle of the atmospheric properties themselves. For a clearer interpretation, we also plot the contribution of $T_a$, $f_c$, and $e_a$ to the seasonal change of Rld in this reply as Fig. R2.

As shown in Fig R1a, the sensitivity of $R_{ld}$ to $T_a$ peaks in the tropics with a maximum of around 5 W/m$^2$/K and decreases at higher latitudes, which is generally consistent with Shakespeare & Roderick (2022). Moreover, the seasonal cycle of the atmospheric properties themselves is shown in the right panel of Figure R1, which reveals that the spatial distribution of the contribution of $T_a$, $e_a$, and $f_c$ to the seasonal variations in $R_{ld}$ (Figure R2) is dominated by the seasonal changes of the air properties (Figs. R1b, R1d, and R1f) instead of the sensitivity of $R_{ld}$ to them (Figs. R1a, R1c, and R1e)."

[Action] We add Fig. R1 to the supplementary information as Fig.S8, put Fig.R2 in the main text as Fig. 5, and add the related analysis to the discussion:

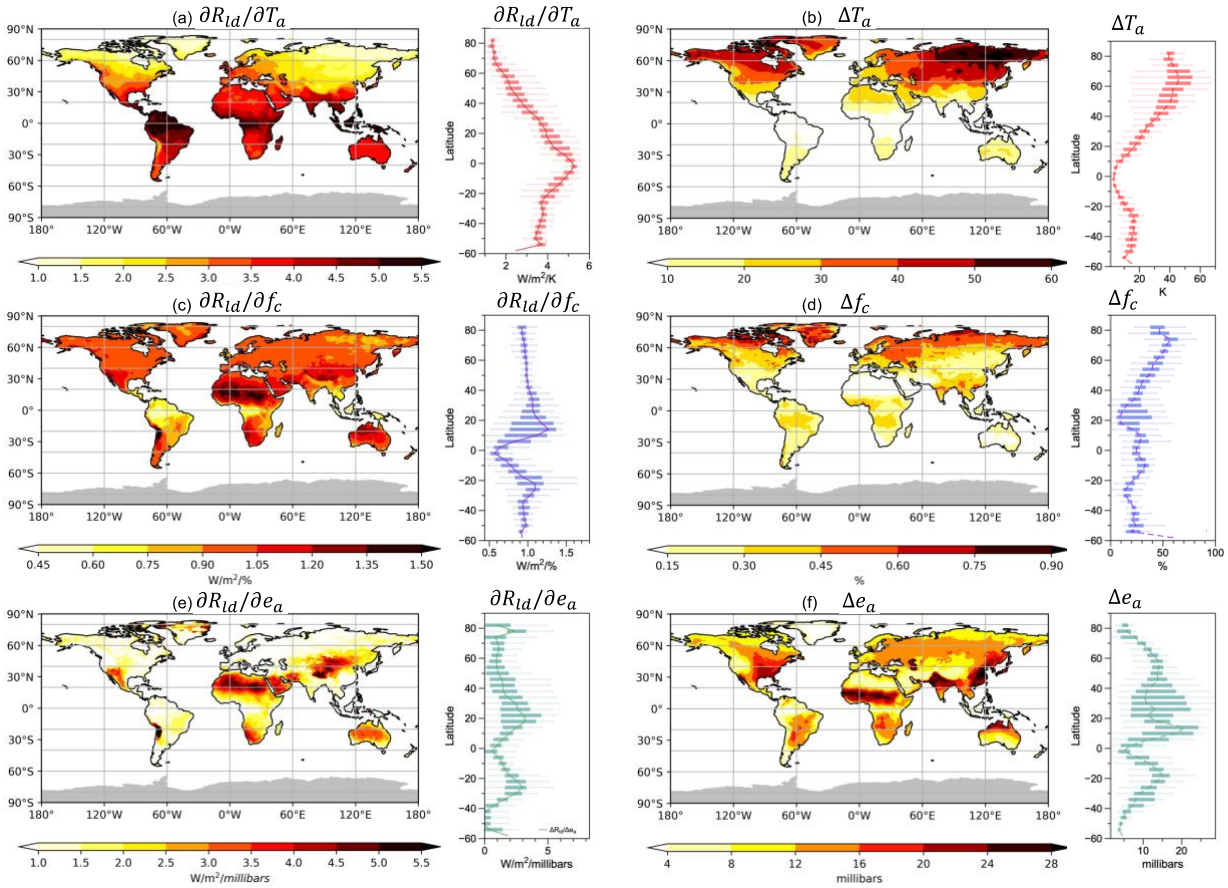


Fig. R1 Distribution of the sensitivity of the seasonal cycle of $R_{ld}$ to surface air temperature ($\frac{\partial R_{ld}}{\partial T} = 4\sigma\bar{\varepsilon}\overline{T_a}^3$) (a), cloud cover ($\frac{\partial R_{ld}}{\partial f_c} = \sigma\overline{T_a}^4 \times \left(1 - \overline{1.24\left(\frac{e_a}{T_a}\right)^{\frac{1}{7}}}\right)$) (c), and water vapor pressure ($\frac{\partial R_{ld}}{\partial e_a} = \sigma\overline{T_a}^4 \times \frac{1.24}{7}\frac{(1-\bar{f}_c)}{(\overline{e_a})^{\frac{6}{7}}(\overline{T_a})^{\frac{1}{7}}}$) ($e$), and their latitudinal variations. Distribution of the seasonal cycle of surface air temperature (b), cloud cover (d), and water vapor pressure (f), and their latitudinal variations. Seasonal cycle ($\Delta$) indicates the difference between the maximum and minimum montly data. In maps, grey shading indicate missing values. In boxplots, the box shows the variation among the land grids at the same latitude, while the solid line is their mean. The upper and lower whisker indicate 95$^{th}$ and 5$^{th}$ percentiles, upper boundary, median line, and lower boundary of the box indicate the 75$^{th}$, 50$^{th}$, 25$^{th}$ quantiles, respectively. Data are from the NASA-CERES dataset.

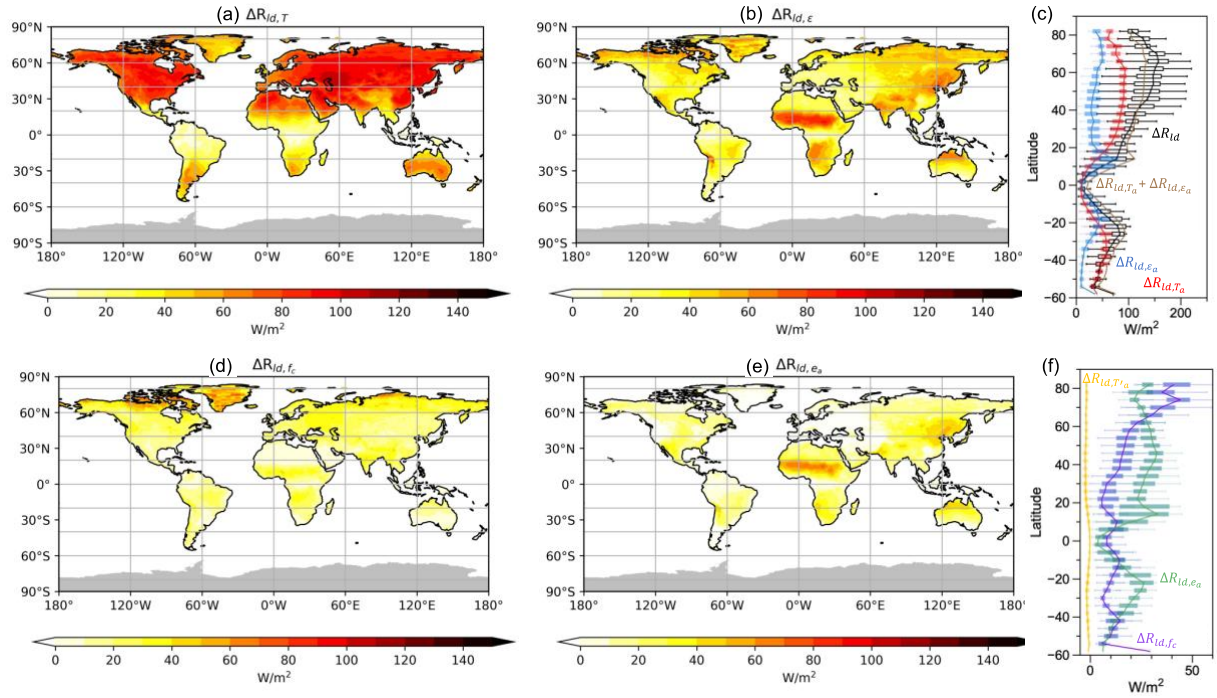


Fig. R2 Decompositions of the mean seasonal variation of $R_{ld}$ (Δ, difference between the maximum and minimum monthly data at each grid) in the NASA-CERES dataset into contributions by lower-level atmospheric heat storage ($\Delta R_{ld,T}$) (a) and emissivity ($\Delta R_{ld,\varepsilon}$) $(b)$, and their latitudinal variations (c). Decomposed of $\Delta R_{ld,\varepsilon}$ into contributions by variations in cloud cover ($\Delta R_{ld,f_c}$) (d) and humidity ($\Delta R_{ld,e_a}$) (e), their latitudinal variations (f). In Figs. a, b, d, e, grey shading indicates missing values. In Figs. c and f, the box shows the variation among the land grids at the same latitude, while the solid line is their mean. The upper and lower whisker indicate 95$^{th}$ and 5$^{th}$ percentiles, upper boundary, median line, and lower boundary of the box indicate the 75$^{th}$, 50$^{th}$, 25$^{th}$ quantiles, respectively.

**Comments**:

1. Figs 1 and 5: This is totally a personal preference, but I don't like diverging colorbars when all the values are positive. I would use a sequential color bar for these figures to contrast them with the bias/difference maps in the rest of the paper.

[Reply] Thank the reviewer for the useful comment. We agree that diverging colorbar may give a wrong interpretation of the figure.

[Action] Using sequential colorbar in Figs. R3 and R2, which are Figs. 1 and 5 in the revised text, respectively.

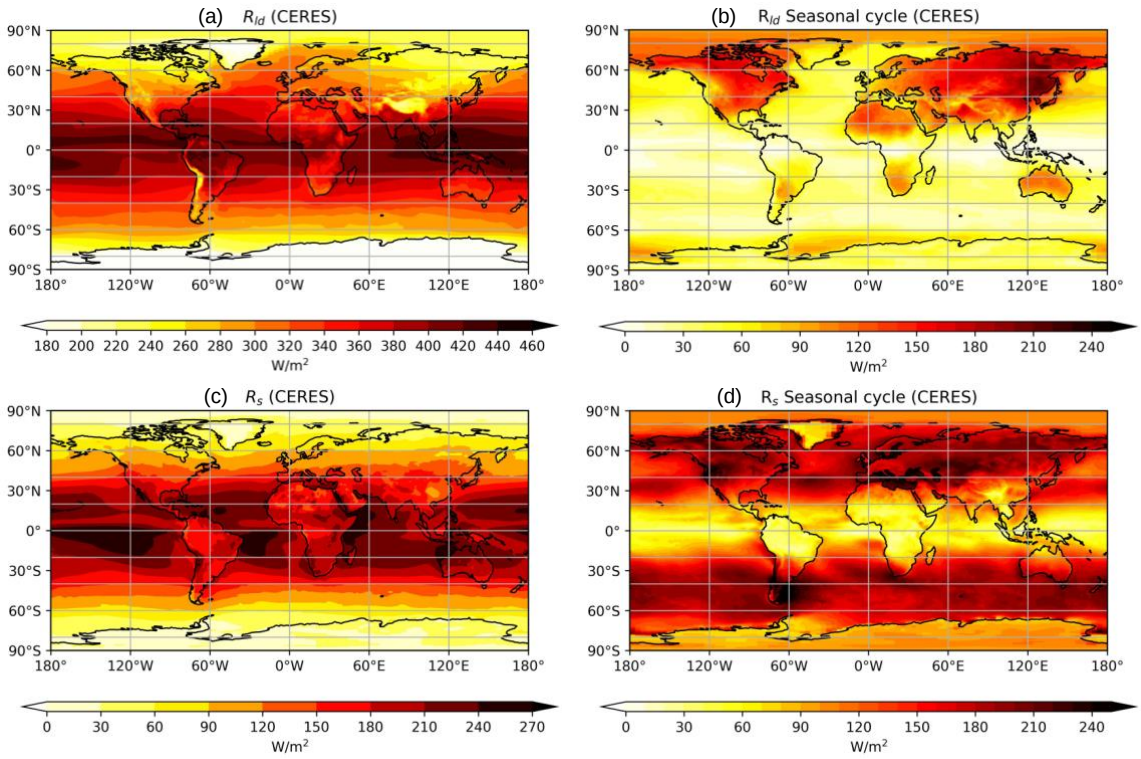


Figure R3. Spatial distribution of the climatological mean (a, c) and the seasonal amplitude (b, d) of downward longwave radiation and absorbed solar radiation at the surface respectively from the NASA-CERES dataset. The seasonal amplitude is calculated as the difference between the maximum and minimum monthly data.

## 2. Line 33: Check if it's the dominant term (isn't surface OLR bigger?)

[Reply] Although the surface Outgoing Longwave Radiation (OLR) is the largest term in the surface energy balance (averaging 396 W/m² globally), we have deliberately chosen not to emphasize it in our discussion. Our focus is on highlighting the energy input in the surface energy balance, primarily comprising downward longwave radiation and absorbed solar radiation.

[Action] Revise the sentence as "*In the global mean surface energy budget, downward longwave radiation ($R_{ld}$) is the dominant surface energy input (333 W/m$^2$), contributing more than twice as much energy as absorbed solar radiation (161 W/m$^2$) (Trenberth et al. 2009)*".

## 3. Line 44: This is a nice description of the development of Brutsaert's Equation, but I'd love for a bit more physical intuition of why we should expect the 1/T_a dependence of the emissivity on temperature.

[Reply] Thank you for the comment. The $1/T_a$ dependence of the emissivity on the temperature in equation 1 largely arises from the way Brutsaert 1975 derives the equation following the assumption of a standard atmosphere. Brutsaert derived the emissivity by integrating

Schwarzschild's equation (equation 2 in B75: ( $F_{LU}, F_{LD}$) $= \int_{a=0}^{\infty} \pi B(T) \frac{\partial \epsilon_0(1.66a,T)}{\partial a} da$)). According to that equation, the emissivity will depend on the scaled amount of water matter ($a$) for a clear sky. The scaled amount of water vapor ($a$) then in turn depends on humidity profiles (equations 3 and 8 in B75: $da = \rho_\omega (p/p_s)^{1/2} dz$ and $\rho_\omega = 0.622 \left(\frac{e_a}{R_d T_a}\right) \exp(-k_\omega z)$). Hence, the term $\frac{e_a}{T_a} dz$ (or $e_a \frac{dz}{T_a}$) is introduced into the Equation, which essentially represents water vapor amount ($e_a$) considering the air volume increases ($T_a$) with temperature ($dz$). As we mentioned, Brutsaert then assumed a standard atmosphere and derived simple expressions for humidity profiles that solely depend on surface temperature ($T_a$) and surface water pressure ($e_a$) (equations 5, 7, and 8 in B75), while the integrated terms related to air volume ($dz$) is replaced by the empirical parameters "1.24" and "1/7".

However, we would like to point out that emissivity is largely insensitive to changes in $\frac{1}{T_a}$ (as demonstrated in the yellow line in Fig. R2f), which has also been acknowledged by B75. In fact, B75 provides another expression of emissivity that solely relies on water-vapor pressure at the surface (Equation 11' in B75: $\epsilon_{a0} = 0.553\ {e_a}^{1/7}$). Moreover, we note that the dependence of $\frac{1}{T_a}$ on emissivity is also hidden in equation 1 due to changes in saturation vapor pressure with temperature. Therefore, it is hard to give a physical description of $\frac{1}{T_a}$ in Eq. 1 directly.

On the other hand, another dependence on emissivity on $T_a$ with physical explanations has been discussed in the current work. Under the freezing point, the emissivity will increase along with decreased temperature (Aase and Idso, 1978), which was not taken into account in B75 and partially contributes to the negative bias observed at low temperatures (Fig. R4a, which is Figure 3 in the revised manuscript).

[Actions]

(1) Following Eq.1, we add a sentence to make the point clear as "*Note that the dependence of* $\varepsilon_{cs}$ *on* $1/T_a$ *shown in Eq.1 should not be overinterpreted considering the derivation of the formula and also the correlation between* $T_a$ *and* $e_a$."

(2) In Figure R2f, we have directly demonstrated the contribution of temperature anomalies to variations in emissivity. However, this contribution is of a smaller magnitude compared to that of cloud and water vapor, and therefore it has received less focus in our work.

(3) We have discussed to effect of temperature on emissivity under the freezing temperature to understand the underestimation of B75 at low temperatures (Fig. R4a) as follows.

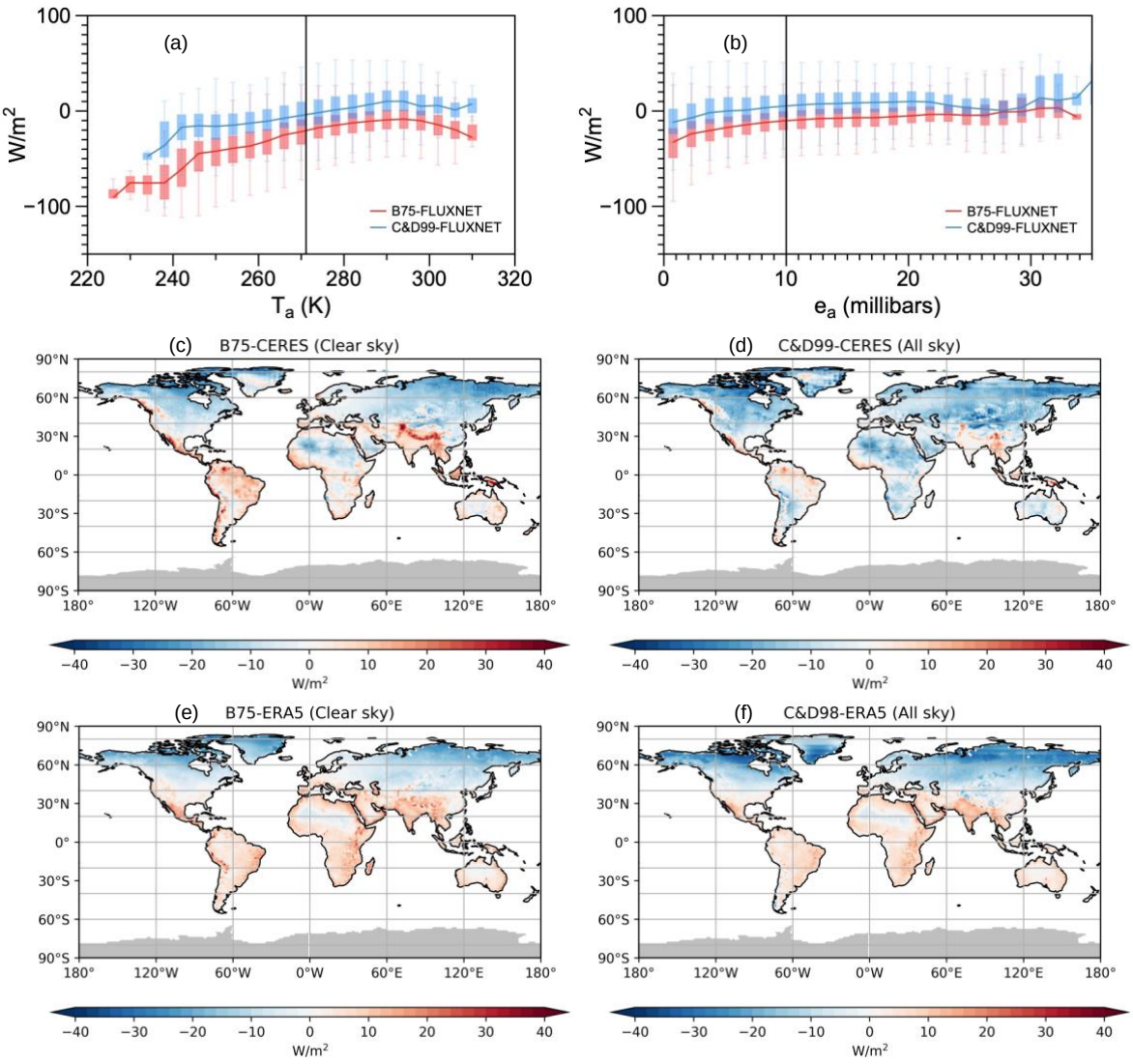


Fig. R4 Biases in the estimates for multi-year mean $R_{ld}$ for FLUXNET data of 189 sites against air temperature (a) and water vapor pressure (b). Distribution of biases in the estimates for multi-year mean $R_{ld}$ for (c, d) NASA-CERES data from 2001 to 2018 and (e, f) ERA reanalysis from 1979 to 2021 for (c, e) clear-sky and (d, f) all-sky conditions over land. Grey shading indicates missing values.

4. Lines 50-51: I understand this equation is empirical, so the units don't have to make sense, but I think you should name the correct units for this equation in your description so readers who want to use this formula immediately know how to apply it. I also assume e_a corresponds to the 2m vapor pressure, but it's not stated explicitly.

[Reply] Thank you for pointing this out.

[Action] We have specified the unit of $e_a$ (millibars) and $T_a$ (K), as well as the definition of $e_a$.

5. Line 62: Can you be specific about what "this" estimate refers to, Is it Eq. 4, or 5?

[Reply] Thanks for pointing out a potential unclarity. “This” refers to Eqs. 4, and 5.

[Action] The sentence is rewritten for better clarity.

6. Lines 105-107: Is the cloud cover fraction from CERES used for all the calculations? If so, what’s the relationship between cloud cover calculated from CERES and the very specific way it is defined in Eq. 3?

[Reply] We sincerely appreciate the reviewer for providing insightful and critical feedback. As shown in Fig. R5, the value derived from Equation 3 generally yields smaller cloud cover fractions compared to those obtained from both the CERES and ERA5 datasets. As a result, when estimating $R_{ld}$ based on Equation 3 under all sky conditions, the error distribution closely resembles that of clear sky conditions (Figures R4c-R4f). Moreover, this discrepancy affects the decomposition of seasonal variations, highlighting a higher contribution of water vapor anomalies to emissivity in tropical regions, particularly the Intertropical Convergence Zone, while cloud cover variations exert a greater influence over high latitudes (Figs. R2).

[Action] We have conducted all our analyses using fc calculated from Equation 3 instead of the cloud cover fraction.

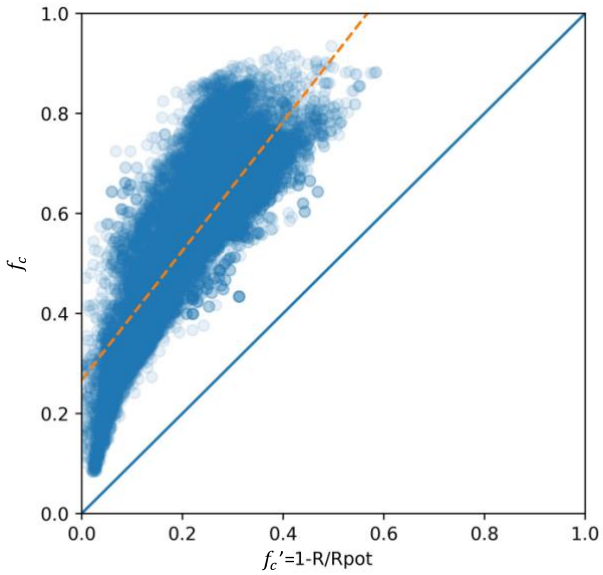


Fig. R5 The scatter plot using the calculated cloud cover fraction (fc’=1-R/Rpot) and cloud cover from CERES datasets (fc). The dashed orange line is the linear regression while the solid blue line delicates the slope of 1.

7. Lines 127-131: Similar to my question about line 44, there’s not much physical explanation for these biases, the authors merely note that Brutsaert also discussed how the equation was

biased for places with big temperature departures away from the global mean. I'm also not sure why the fact that the biases are less than the seasonal cycle is relevant.

[Reply] As mentioned in our response to comment #3, the underestimation observed at low temperatures, particularly near and below the freezing point, in Brutsaert's equation is attributed to its failure to account for the increase in Rld with decreasing temperatures below 0 ℃, as discussed in Aase and Idso (1978). It is worth noting that the biases identified, despite their presence, are smaller in magnitude compared to seasonal variations. Consequently, these biases do not hinder our utilization of the Brutsaert equation to attribute the causes behind seasonal variations.

[Action] In order to further enhance our understanding of the errors in B75, we have included this physical explanation in our work as follows: "*Moreover, B75 has not considered the gradual increase in emissivity as temperature decreases below freezing (Aase and Idso 1978), thus explaining the underestimation under low temperature (Figs. 3b, S3b, S3b). The biases seen in Figure 3 are nevertheless notably smaller than the spatial-temporal variations shown in Figure 1, this means that these biases do not prevent us from using Brutsaert to attribute the causes for the seasonal variation and the spatial range of* $R_{ld}$."

8. Lines 132-135: Could the consistent positive bias in the all-sky calculation be driven by the cloud fraction definition related to my comment on lines 105-107? I think the definition of cloud fraction in these equations is pretty important to potential biases.

[Reply] Yes, the consistent positive bias in the all-sky calculation was driven by the way cloud fraction was defined from CERES. After repeating the analysis using a new metric of cloud-fraction as described in C&D 99, we found that the consistent positive bias in the all-sky calculation cannot be detected anymore (as shown in Fig. R4). We thank the reviewer for pointing this out.

9. Fig 3: Can you also show the biases from the AMERIFLUX dataset? Do those biases line up with the expectations from the global datasets?

[Reply] Thank you for this comment, which helps to justify our related statement.

[Action] Since the FLUXNET stations are primarily located in America and Europe, interpreting errors on the map figure becomes challenging. To address this, we have directly showcased the biases derived from the FLUXNET dataset alongside temperature and water vapor pressure (Figs. R4a-R4b), which demonstrates consistent patterns with the CERES and ERA5 datasets (Fig. R6, which is Fig. S3 in the supplementary material).

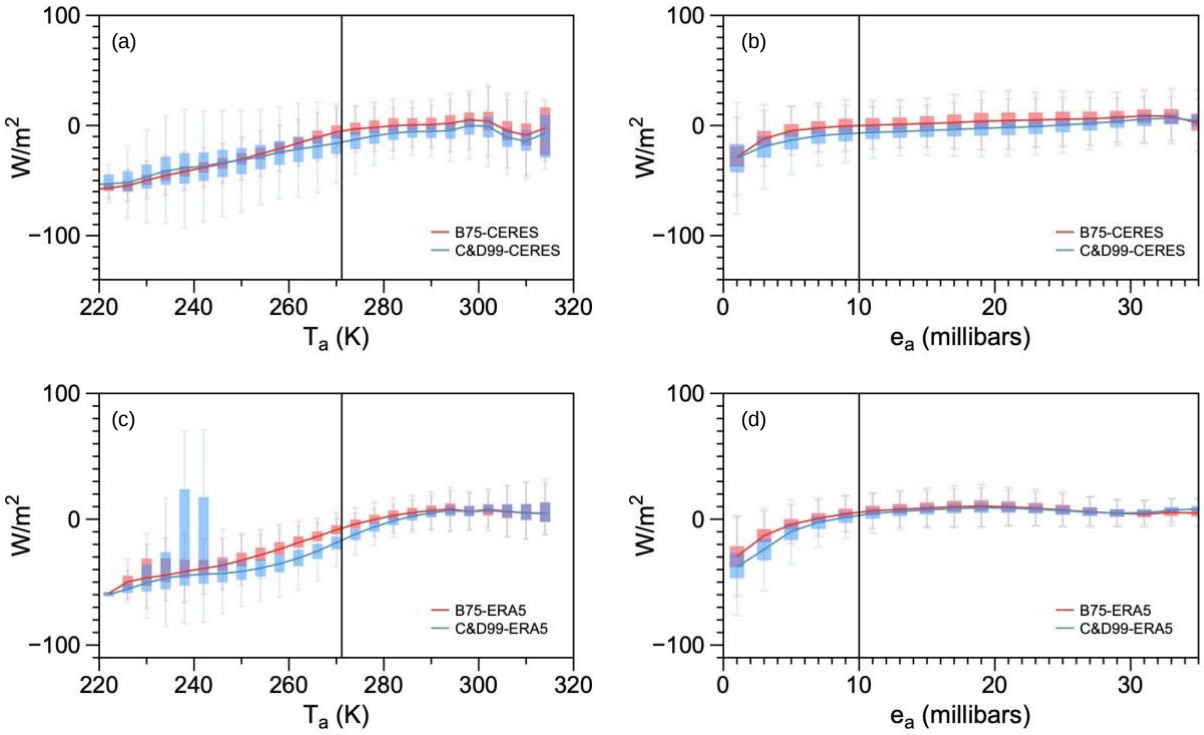


Figure R6. The same as Figs. R4a and R4b but with data from ERA5 (a and c) and CERES data (b and d)

10. Line 147: Is it small compared to or just small compared to from the Stephan Boltzman law? Are the water vapor and temperature components from the the emissivity equation of the same order of magnitude? If so, I think both temperature terms should be included.

[Reply] Although the pictures of the two equations in the comment are not available from our side, most likely due to a website issue, we assume that the reviewer is interested in understanding to which extent temperature variation contributes to the change in emissivity ($\Delta R_{ld,T_a'} = \sigma\overline{T_a}^4 \times (-\frac{1.24}{7}) \times \frac{(1-\bar{f}_c)(\overline{e_a})^{\frac{1}{7}}}{(\overline{T_a})^{\frac{8}{7}}} \times \Delta T_a$). This term is of less order than those of cloud ($\Delta R_{ld,f_c} = \sigma\overline{T_a}^4 \times \left(1 - 1.24\left(\frac{e_a}{T_a}\right)^{\frac{1}{7}}\right) \times \Delta f_c$) and water vapor ($\Delta R_{ld,e_a} = \sigma\overline{T_a}^4 \times \frac{1.24}{7} \frac{(1-\bar{f}_c)}{(\overline{e_a})^{\frac{6}{7}}(\overline{T_a})^{\frac{1}{7}}} \times \Delta e_a$),which are in turn of less order than the contribution of atmospheric storage ($\Delta R_{ld,T_a} = \varepsilon_a \sigma\overline{T_a}^3 \times \Delta T_a$).

[Action] in the revision, we have substantiated this statement with Fig. R2f.

11. Lines 166-169: The monsoonal regions really stick out as having a sizable water vapor control on DLR. Even though the cloud cover causes changes in seasonal cycle strength, the

ultimate cause is changing water vapor or monsoonal circulation patterns, and I think this should be noted.

[Reply] Considering the substitution of the cloud cover fraction with the value calculated from Eq.3, the decomposition analysis has been impacted.

[Action] Consequently, we have conducted a reanalysis of the relevant data, revealing a noteworthy influence of water vapor on downward longwave radiation (DLR) over the Intertropical Convergence Zone (ITCZ) and monsoon regions (Fig. R2).

12. Lines 183-187: I'm confused about what's being plotted in Fig. 6a-d. Are these departures from the global mean that includes the ocean or just the terrestrial global mean?

[Reply] We apologize for not making it clear. It is the departure from the terrestrial global mean.

[Action] It has been made clearer in the caption as "***Figure 6.*** *The decomposition of the annual-mean spatial variations (Δ, departure from the terrestrial global mean) of in the NASA-CERES dataset into contributions by (a) atmospheric heat storage* ($\Delta R_{ld,T}$) *and (b) emissivity* ($\Delta R_{ld,\varepsilon}$). *The variations in* $\Delta R_{ld,\varepsilon}$ *are further decomposed in contributions by variations in (c) cloud cover* ($\Delta R_{ld,f_c}$) *and (d) humidity* ($\Delta R_{ld,e_a}$)."

13. Line 195: 20W/m2 across the entire aridity index spectrum.

[Reply] Thank you for this detailed comment.

[Action] We have incorporated it into the text.

**Reference:**

Aase, J. K., and S. B. Idso, 1978: A comparison of two formula types for calculating long-wave radiation from the atmosphere. Water Resources Research, 14, 623-625. https://doi.org/10.1029/WR014i004p00623

Shakespeare C. J. and M. Roderick. (2022). Diagnosing Instantaneous Forcing and Feedbacks of Downwelling Longwave Radiation at the Surface: A Simple Methodology and Its Application to CMIP5 Models. Journal of Climate.

Vargas Zeppetello, L. R., Donohoe, A., & Battisti, D. S. (2019). Does surface temperature respond to or determine downwelling longwave radiation? Geophysical Research Letters, 46, 2781–2789. https://doi.org/10.1029/2019GL082220